Potential-Based Modeling of 2-D Regions Using Nonuniform Source Distributions

Jen-Hui Chuang, Chi-Hao Tsai, Wei-Hsin Tsai, and Chuei-Yaw Yang

***Abstract*—One of existing approaches to path planning problems uses a potential function to represent the topological structure of the free space. Newtonian potential was used in [1] to represent object and obstacles in the two-dimensional (2-D) workspace wherein their boundaries are assumed to be uniformly charged. In this paper, more general, nonuniform distributions are considered. It is shown that for linear or quadratic source distributions, the repulsion between two polygonal objects can be evaluated analytically. Simulation results show that by properly adjusting the charge distribution along obstacle/object boundaries, path planning results can be improved in terms of collision avoidance, path length, etc.**

***Index Terms*—Collision avoidance, nonuniform source distributions, path planning, potential fields.**

I. Introduction

The goal of path planning is to determine how to move an object from its original location and orientation (called the starting configuration) to the goal configuration while avoiding any collision with obstacles. The configuration space (c-space) approaches [2]–[6] consider both the object and known obstacles at the same time by identifying object configurations (points in the c-space) intersecting the obstacles. The path planning problem is thus transformed into a problem of finding a collision-free path of a point object in the c-space.

While the geometry of the moving object has to be taken into account from the very beginning of path planning algorithms for the c-space approaches, workspace-based algorithms often work differently and consist of two parts. In the first part, relevant information about the free space is extracted, which is then used together with the object geometry in the second part to find a path. Usually, the free space is decomposed into simpler cells [7] or divisions [8]–[10], and possibly with associated weights [11]. In addition, the object geometry can be approximately represented by primitives of simple shapes [12], [13].

The above algorithms do not always choose the object configurations which best match the shape of the free space along a path. One way to obtain the best match and minimize the risk of collision is to define a repulsive potential field between the object and the obstacles. Such a potential field can itself serve as a representation of free space. A cubic function of the distance between a point object and the obstacles is used in [14] as the potential function. An artificial repulsive potential which is the function of the shortest distance between the moving object and the obstacles is used in [15] for local planning of linked line segments. Similar local planning is done in [16] using a superquadric artificial potential function whose isopotential contours are modified n-ellipses and the potential values are determined by the Yukawa function [17]. Boundary equations of polytopes are used in [18] to create an artificial potential function. A sliding mode control strategy for tracking the gradient of an artificial potential field is introduced in [19]. The main advantages of the potential-based approaches include the simplicity of the representation of free space, the guidance in the object motion provided by the negation of the potential gradient in the form of repulsive force and torque, and the readiness of the extension to spaces of higher dimensions (see [20]).

The Newtonian potential is used in [1] to model the free space wherein the boundaries of object and obstacles are assumed to be uniformly charged. The magnitude of the potential is unbounded near the obstacle boundary and decreases with range, which captures the basic requirement of collision avoidance. In this paper, the above potential model is generalized such that nonuniform source distributions along polygonal boundaries are considered. In Section II, basic properties of the proposed free space model are obtained by examining the potential contours due to some nonuniform source distributions on simple polygonal region borders. In Section III, the repulsion experienced by an object of finite size due to the potential gradient is considered. It is shown that the repulsion between polygonal object and obstacles, in forms of force and torque, can be derived in closed form for linear and quadratic source distributions. Path planning applications of these analytic results are considered in Section IV for local object paths near free space bottlenecks. Simulation results show that, compared with an object path generated using the uniform distribution, a more desirable object path can be obtained by properly adjusting the nonuniform source distribution along object/obstacle boundaries. Section V presents some concluding remarks.

II. Potential due to Some Nonuniform Source Distributions on Polygonal Region Borders

Polygonal description of obstacles is often used in path planning because of its simplicity. The potential due to a polygonal region whose border is uniformly charged can be derived in closed form. It is shown in [1] that planning a path among obstacles thus modeled will guarantee collision avoidance as the potential will increase indefinitely as an object approaching an obstacle. In this paper, such a potential-based approach is generalized to take into account some nonuniform source distributions.

While the uniform distribution works satisfactorily in terms of collision avoidance, further improvements are possible for an object path thus obtained. For example, a sharp corner of an object often gets closer to obstacles than a dull one, and has a higher likelihood of collision, which are not desirable in most cases. In addition, there may be other findpath considerations, e.g., minimum path length, which require more flexible workspace model instead of the one based on the uniform source distribution. On the other hand, there could be certain path planning-related properties of workspace and object which are nonuniform along their boundaries in general and can be modeled better with nonuniform source distributions.

In general, any nonuniform distributions can be approximated by polynomial functions of sufficient order. However, since lower-order polynomials are special cases of the higher-order ones and require less computation, it is desirable to use the lower-order ones whenever possible. In this paper, linear and quadratic distributions are selected as examples of nonuniform distributions because of their simplicity. With these simple distributions, we will be able to address, to some extent, several questions of interest to path planning which include the following:

1) How can path planning results obtained with uniform distribution be improved with the nonuniform ones?
2) What may be the desirable effects on path planning which are achievable with the higher order distributions but not the lower-order ones?

To assess the proposed model at its efficiency, we will first determine if the repulsive potential due to polygonal object boundaries modeled

Manuscript received October 23, 1997; revised October 31, 1999. This work was supported by the National Science Council, R.O.C., under Grant NSC85-2213-E-009-126. This paper was recommended by Associate Editor R. A. Hess.

The authors are with the Department of Computer and Information Science, National Chiao-Tung University, Hsinchu 30056, Taiwan, R.O.C.

Publisher Item Identifier S 1083-4427(00)01729-X.

by these nonuniform distributions, like those due to the uniform one, are also analytically tractable. Since the potential due to a polygonal region with charged border can be calculated by superposing the potential due to individual border segment, only the potential due to a single line segment is formulated in the following.

A. Uniform Source Distribution

The derivation of the potential due to the uniform charge distribution is mentioned in [1], which can also be found in an ordinary textbook on electromagnetics. In the xy-plane, consider a point A at (x_0, y_0) and a charged line segment on x-axis with a unit charge density between $x = x_1$ and $x = x_2$. The potential at point A due to a point $(x, 0)$ of the line segment is equal to

$$V_x = \frac{1}{r} \tag{1}$$

where $r = \sqrt{(x - x_0)^2 + y_0^2}$. The total potential at point A due to the charged line segment is equal to

$$V_A = \int_{x_1}^{x_2} \frac{1}{r}\, dx. \tag{2}$$

B. Linear and Quadratic Source Distributions

Suppose the charge density increases (decreases) quadratically with x from x_1 to x_2, the charge density function can be expressed as $\alpha x^2 + \beta x + \gamma$ with some constants α, β, and γ, and the total potential at the point A due to the charged line segment is equal to

$$V_A = \int_{x_1}^{x_2} \frac{\alpha x^2 + \beta x + \gamma}{r}\, dx. \tag{3}$$

It can be shown that (3) can be evaluated analytically.[1]

In the above discussion, we have considered the uniform, linear, and quadratic charge distributions along a line segment. For polygonal regions with charged borders, the resultant potential can be obtained according to the superposition principle. For example, the equipotential contours due to uniform and some quadratic charge distributions on a *square* are shown in Figs. 1 and 2, respectively. The charge densities are increased quadratically from the midpoint of each edge toward the corners of the square for Fig. 2. Note that as one moved toward a corner of the square, from the outside along the diagonal direction, the potential increases with a higher rate in Fig. 2(b) than in Fig. 1(b), a more desirable property for collision avoidance of an object path.

Although the potential value can be used in the search for object configuration of minimal potential, more efficient search methods can be adopted if the gradient of the potential, which contains the information about how the potential varies, can be obtained. Such potential gradient results in the repulsion between object and obstacles, in forms of repulsive force and torque. In the following section, it is shown that the repulsion between charged object and obstacle boundaries due to different source distributions is analytically tractable.

III. Integral Equations of the Repulsion Due to the Potential Models

For polygonal object and obstacles in the two-dimensional (2-D) space, line segments of their boundaries can be used as basic elements in the calculation of repulsive force and torque needed in path planning.

[1]A linear distribution corresponds to $\alpha = 0$.

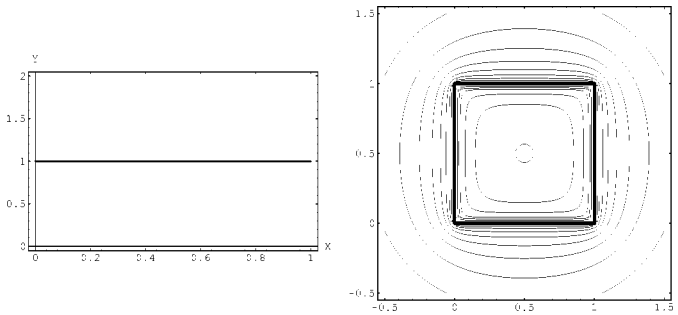

(a) (b)

Fig. 1. Potential contours due to a charged square boundary. (a) The charge distribution on each edge of the square. (b) The resultant equipotential contours.

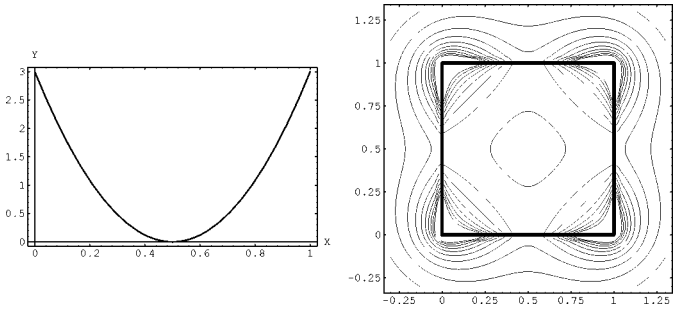

(a) (b)

Fig. 2. Potential contours due to a charged square boundary. (a) The charge distribution on each edge of the square. (b) The resultant equipotential contours.

The repulsive force and torque between these polygonal regions can then be derived by superposing the repulsion between pairs of border segments, each contains one line segment from the moving object and the other from one of the obstacles.

In general, each pair of the repelling line segments can have arbitrary configuration in the work space as shown in Fig. 3(a). To simplify the expressions of the repulsion between them in the following subsections, a coordinate system is chosen so that the obstacle line segment, $\overline{AB}$, lies on the base line, as shown in Fig. 3(b). In the new coordinate system (uv-plane), the coordinates of the endpoints of $\overline{AB}$ are assumed to be $(0, 0)$ and $(d > 0, 0)$, respectively, and the line containing the object line segment, $\overline{CD}$, can be represented as $v = au + b$, $u_1 \le u \le u_2$.

A. The Integral Equations for Forces

Consider the electric field at point $Q = (u', v')$ of $\overline{CD}$ due to a point $(u, 0)$ on $\overline{AB}$ shown in Fig. 3(b), we have

$$\vec{E} \triangleq (E_u, E_v) = -\nabla \left[\frac{1}{r}\right] = -\frac{1}{r^2}\hat{r} \tag{4}$$

where $\vec{r} = (u' - u, v')$, $r = |\vec{r}| = \sqrt{(u' - u)^2 + v'^2}$, and $\hat{r} = \vec{r}/r$. Thus, the total force $\vec{F}(u', v')$ at point Q due to $\overline{AB}$ can be decomposed into two parts, i.e.,

$$F_u(u', v') = \int_{q_1}^{q_2} E_u\, dq = \int_0^d \frac{u' - u}{r^3}\rho(u)\, du \tag{5}$$

$$F_v(u', v') = \int_{q_1}^{q_2} E_v\, dq = \int_0^d \frac{au' + b}{r^3}\rho(u)\, du \tag{6}$$

where $\rho(u)$ is the charge density along $\overline{AB}$.

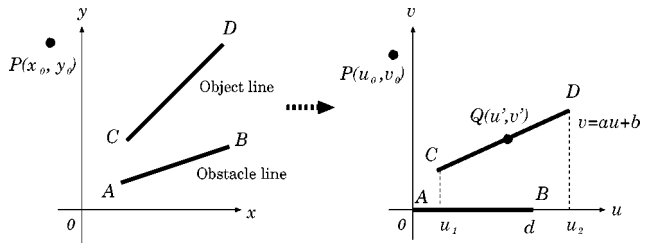

(a) (b)

Fig. 3. Coordinate transformation. (a) The original coordinate system (xy-plane). (b) The new coordinate system (uv-plane) after the transformation.

For the total force on object line segment $\overline{CD}$, we have[2]

$$F_u = \int_{q_1}^{q_2} F_u(u', v')\, dq = \int_{s_1}^{s_2} F_u(u', v')\rho(s)\, ds \tag{7}$$

where $s = \sqrt{1+a^2}u'$, $\rho(s)$ is the charge density along $\overline{CD}$, and $dq = \rho(s)\, ds = \sqrt{1+a^2}\rho(u')\, du'$. Thus, the above integral equations can be formulated as

$$F_u = \sqrt{1+a^2}\int_{u_1}^{u_2}\int_0^d \frac{u'-u}{r^3}\rho(u)\rho(u')\, du\, du' \tag{8}$$

B. The Integral Equations for Torques

Given any collision-free orientation of an object with nonzero torque with respect to its rotation center, the direction of the torque directly gives the direction in which the object should rotate to reach a configuration of smaller potential. In this subsection, we will consider the formulation of the repulsive torque between two charged line segments. Consider $\overline{AB}$ and $\overline{CD}$ shown in Fig. 3(b) and let $P = (u_0, v_0)$ be a reference point, e.g., the rotation center of the object. The torque with respect to P, due to the repulsive force from $\overline{AB}$ on point Q is equal to

$$\begin{aligned}\tau_P(u', v')\vec{i_z} &= \vec{l}(u', v') \times \vec{F}(u', v') \\ &= (u'-u_0, v'-v_0) \times (F_u(u', v'), F_v(u', v'))\end{aligned} \tag{9}$$

where $\vec{i_z} = \vec{i_u} \times \vec{i_v}$ and $\vec{l}(u', v') = \vec{PQ} = (u'-u_0, v'-v_0)$. Thus, the total torque with respect to P due to the repulsion between the two line segments becomes

$$\begin{aligned}\tau_P &= \int_{s_1}^{s_2} \tau_P(u', v')\rho(s)\, ds \\ &= \sqrt{1+a^2}\left(\int_{u_1}^{u_2}\int_0^d (u'-u_0)\frac{au'+b}{r^3}\rho(u)\rho(u')\, du\, du' \right. \\ &\quad \left. - \int_{u_1}^{u_2}\int_0^d (au'+b-v_0)\frac{u'-u}{r^3}\rho(u)\rho(u')\, du\, du'\right)\end{aligned} \tag{10}$$

We will now show that with the above integral equations, the repulsive forces and torques between object and obstacles can be evaluated analytically for some simple nonuniform charge distributions along their boundaries.

C. Repulsion Due to Simple Charge Distributions

For the application of the proposed potential model in achieving collision avoidance in path planning, the optimal object configurations along a path can be found more efficiently if the above integral equations can be evaluated analytically instead of numerically. The main advantage of the proposed model is that such analytic expressions exist for the simple charge densities considered in this paper.

Assume the charge density $\rho(u)$ is equal to 1, u, or u^2 for an obstacle line, and $\rho(s) = 1$, s, or s^2 for an object line, nine different combinations of charge distributions will need to be considered in evaluating the repulsion between the two line segments. For example, from (8), the repulsive force along the u-axis for these nine combinations can be obtained from

$$\begin{aligned}F_u^{ij} &\triangleq F_u^{ij}(u_2) - F_u^{ij}(u_1) \\ &= (1+a^2)^{\frac{j+1}{2}}\int_{u_1}^{u_2}\int_0^d \frac{u'-u}{r^3}u^i\, du(u')^j\, du'\end{aligned} \tag{11}$$

where i is equal to the order of the charge density of the obstacle line, and j is equal to that of the object line. It can be shown that analytic expressions exist for all these integral equations. For example, we have

$$F_u^{00}(u_1) = \log\frac{f_1'(u_1)/2 + \sqrt{1+a^2}f_1^{1/2}(u_1)}{f_2'(u_1)/2 + \sqrt{1+a^2}f_2^{1/2}(u_1)} \tag{12}$$

where $f_1(u) = (au+b)^2 + (u-d)^2$ and $f_2(u) = (au+b)^2 + u^2$.

In general, $\rho(u)$ and $\rho(s)$ can be any quadratic functions

$$\rho(u) = \alpha_1 u^2 + \beta_1 u + \gamma_1 \tag{13}$$

$$\rho(s) = \alpha_2 s^2 + \beta_2 s + \gamma_2 \tag{14}$$

where coefficients $\alpha_1, \beta_1, \gamma_1, \alpha_2, \beta_2$, and γ_2 are some real numbers. The repulsive force along the u-axis can still be evaluated analytically as

$$\begin{aligned}F_u = {} & \alpha_1\alpha_2 F_u^{22} + \alpha_1\beta_2 F_u^{21} + \alpha_1\gamma_2 F_u^{20} \\ & + \beta_1\alpha_2 F_u^{12} + \beta_1\beta_2 F_u^{11} + \beta_1\gamma_2 F_u^{10} \\ & + \gamma_1\alpha_2 F_u^{02} + \gamma_1\beta_2 F_u^{01} + \gamma_1\gamma_2 F_u^{00}.\end{aligned} \tag{15}$$

Similar results can be obtained for F_v and τ_P. Thus, for any $\rho(u)$ and $\rho(s)$, we can first evaluate the coefficients of the charge density functions and then use the nine sets of expressions of the repulsion, as in (15), to evaluate the total repulsion.

IV. Application of the Potential Model in Path Planning

In the previous section, it is shown that the repulsion between two polygonal regions, in forms of repulsive force and torque, can be evaluated analytically. In this section, the above results will be used to ensure collision avoidance in path planning for polygonal object and obstacles in the 2-D space.

A. A Local Planning Algorithm

For a path planning problem, the places where the moving object is more likely to collide with obstacles are bottlenecks in the free space. In the 2-D space, free space bottlenecks can be defined by the minimal distance links (MDL's) among obstacles. For example, MDL's are used to connect (convex) obstacle nodes in the obstacle neighborhood graph in [10]. Central to the solution to the path planning problem is the identification of the set of bottlenecks in the free space to be traversed by the object in order to reach the destination.

In this section, a simple local planner (similar to that presented in [1]) is used to demonstrate one possible application of the proposed potential model to path planning, i.e., the identification of optimal object configurations (each has minimum likelihood of collision with respect to the potential function) along the local path around a bottleneck. The

[2]For simplicity, only the u-component is considered for the rest of the paper.

topology of a local path, given as input to the local planner, is described in terms of the associated MDL and the object skeleton[3]. The description is of a very concise form which only specifies the sequence in which the skeleton points should cross the MDL. If such a description corresponds to a feasible object path, the local planner will generate a sequence of object configurations along the path, each of minimum potential; otherwise, a failure will be reported.

Let s_i, $1 \leq i \leq N$, denote the sequence of N selected skeleton points to cross the MDL while L denotes the line containing the MDL. The local path begins when s_1 reaches the MDL and ends when s_N leaves the MDL. The following algorithm developed for the local planner performs the path planning by sequentially ensuring that as each skeleton point moves onto the MDL, it stays on L while the location and orientation of the object is adjusted to minimize the Newtonian potential using repulsive torque (**T**) and force (**F**) experienced by the object. Additional skeleton points may be added (see algorithm) to reduce the step size along the path, allowing for finer adjustments in the object configuration to avoid collision. To restrict the total amount of computation, a limit is put on the minimum spacing $s_{\min}$ between adjacent skeleton points used in the simulation, which effectively serves as a feasibility test of the local plan.

ALGORITHM *LOCAL_PLAN*:

Step 0: (Begin with the first skeleton point)
Initialize $i = 1$.

Step 1: (For this skeleton point, find the minimal potential object configuration)
Shift the object parallel to L and rotate it with respect to s_i until **T** and the projection of **F** along L are both zero.

Step 2: (End when done with the last skeleton point)
If $i = N$, the local planning is completed.

Step 3: (Translate the next skeleton point onto MDL if possible)
Translate the object such that s_{i+1} is shifted to its projection on L. If there is no collision during the translation, then let $i \leftarrow i + 1$, and go to Step 1.

Step 4: (Translate an intermediate skeleton point onto MDL)
Find the smallest $n \geq 1$ such that $s_i' = s_i + (s_{i+1} - s_i)/2^n$ can be shifted to its projection on L without collision between the object and obstacles. If $|s_i' - s_i| > s_{\min}$, then let $s_i \leftarrow s_i'$, and go to Step 1.

Step 5: (End abnormally)
Exit with failure due to the need for less than allowed spacing of skeleton points.

An object configuration obtained in Step 1 is not only collision-free but also the safest with respect to the Newtonian potential under the constraint that the corresponding skeleton point stays on L. Such a minimal potential configuration always exists for s_i located on the MDL which connects two obstacles. For the implementation of Step 1, the minimal potential configuration is identified efficiently by performing two binary searches: one for the object location using **F** and the other for the object orientation using **T**. The accuracies required for specifying the final object location and orientation determine the number of iterations needed for solving the corresponding constrained optimization problems. For the simulation results presented in the next subsection, the minimal potential configurations are specified to within 1% of the length of the MDL in location, and within one degree in orientation. In Steps 3 and 4, the swept volume of the object due to the translation is checked for possible intersection with all obstacle regions to detect a collision.

[3]The identification of the sequence of MDL's (or similar constraints) for a global path, as well as the selection of a sequence of skeleton points of the object (whose skeleton may even have a branch) for each local path, are beyond the scope of this paper.

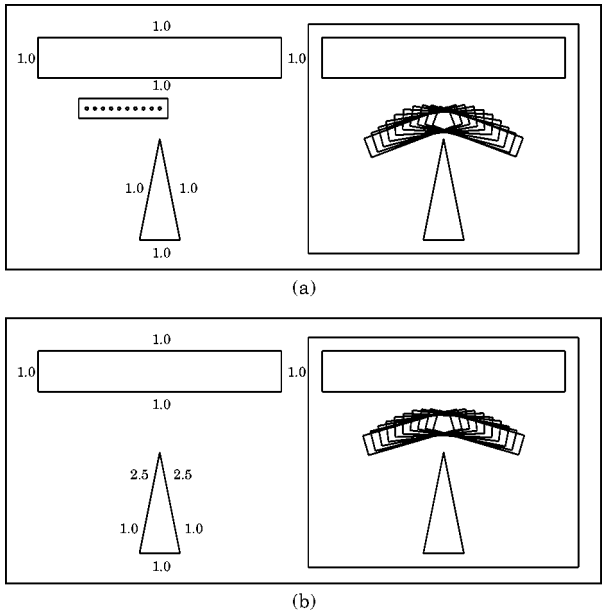

Fig. 4. A path planning example. The obstacle boundaries are (a) uniformly charged, (b) nonuniformly charged.

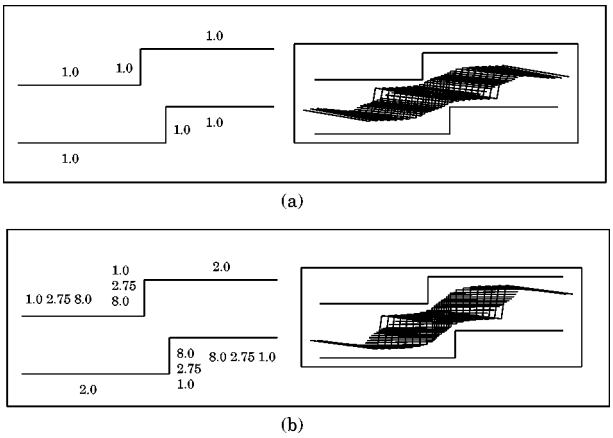

Fig. 5. Path planning example. The obstacle boundaries are (a) uniformly charged, (b) nonuniformly charged.

B. Simulation Results

In this subsection, simulation results are presented for path planning of objects with uniformly charged boundary for simplicity. In addition to planned object paths, in order to make easy the observation of different charge distributions along obstacle boundaries, values of the charge density function for different locations along each boundary segment are also displayed. Thus, to each segment, one, two or three numbers will be attached in the illustration depending on whether the corresponding charge density function is of zero, first or second order, respectively. While values of the charge density are displayed for the two endpoints of a linearly charged segment, the density is also displayed for the midpoint of a quardratically charged segment.

Figs. 4 and 5 show local planning results for several object paths. (For simplicity, skeleton points are only shown for the object in Fig. 4.) The paths obtained with *LOCAL_PLAN* are safe and smooth because the potential function are spatially smooth and maximum freedom is allowed in the adjustment of the object configuration to achieve minimum potential. Different effects of changing the charge distributions along obstacle boundaries can be observed. In general, by properly

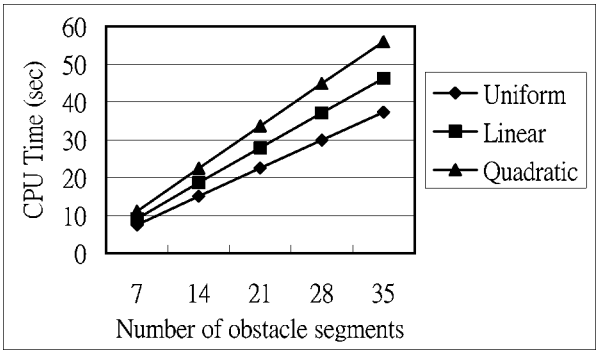

Fig. 6. CPU times spent in obtaining path planning results similar to that shown in Fig. 4.

readjusting the originally uniform charge distribution, the minimum distance between an object path and obstacles can be reduced. For example, such an effect can be achieved if more charges are added to protruding points of the obstacles.

On the other hand, the computing cost is higher if higher-order charge distributions are adopted in the simulation because the associated force and torque calculations are more complex. Fig. 6 shows the CPU times spent in obtaining path planning results similar to that shown in Fig. 4. While the obstacle boundaries are uniformly charged, as in Fig. 4(a), three sets of simulation results are obtained for different charge distributions along the object boundary, and for different numbers of obstacle segments as well.[4] In order to simplify the analysis, all the object border segments are charged with source distributions of the same order for each set of the data. For a given number of obstacle segments, the increase in the computing cost due to the increase in the order of the charge distribution is readily observable.[5] Also note that for each set of data, the computing cost increases linearly with the number of obstacle segments. Such a result is a direct consequence of the fact that the force and torque calculations are required for each pair of object-obstacle segments.

Figs. 7–9 show path planning examples involving multiple local paths. For each of the examples, the local paths are so close to their neighbors along the global path that the union of them constitutes a reasonable object path. [6]. Also note that only one skeleton point of the object, its centroid, is used by the local planner for these examples. In Fig. 7, local paths are obtained for a sequence of vertical obstacle links between two parallel obstacle segments of a straight passage. A curved object path is obtained in Fig. 7(b) since extra charges are added near the midpoint of only one side of the passage. Such an example demonstrates the possibility of the proposed potential-based modeling of the workspace to accommodate certain path planning constraints/considerations of interest, e.g., building material, protection measure, or uncertainty in location (see [21]), which are generally nonuniform along workspace boundaries.

In Fig. 8, a sequence of vertical obstacle links are used for a zigzag passage along the horizontal direction. Fig. 8(a) and (b) shows object paths obtained by using uniform and linear source distributions, respectively. No matter how its parameters are modified, the linear distribution always results in a wavy appearance of the object path. On the other hand, a near straight object path, i.e., a path of minimum length, can

[4]The number of obstacle segments are increased by duplicating those segments.

[5]Such an increase in computing cost may not be a problem if, as the case considered in this paper, the order of the charge distribution of interest is small.

[6]For brevity, considerations for situations when such a condition is not satisfied that additional processes may be required to connect the local paths are omitted. One way of performing the connecting task can be found in [1]

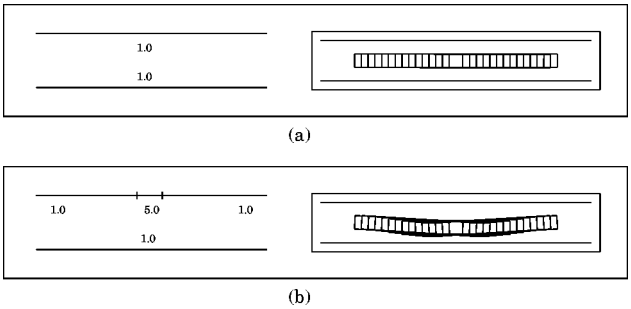

Fig. 7. Path planning example. The obstacle boundaries are (a) uniformly charged, (b) nonuniformly charged.

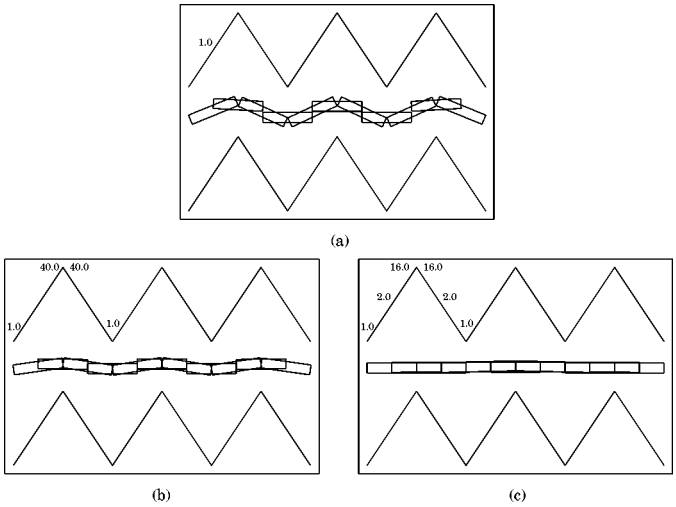

Fig. 8. Path planning example. The obstacle boundaries are (a) uniformly charged, (b) linearly charged, and (c) quadratically charged.

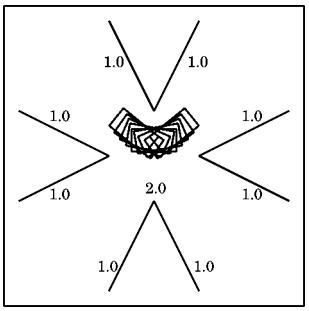

Fig. 9. Path planning for an object among more than two obstacles.

be obtained with the quadratic distribution shown in Fig. 8(c). Such a result is due to the fact that in order to generate near horizontal equipotential contours in the vicinity of the centerline of the zigzag passage, a higher degree of unevenness in the source distribution, which is feasible with the quadratic distribution but not with the linear one, is required. In Fig. 9, it is assumed that three of the six MDL's among the four obstacles, which are connected to a common obstacle vertex, are selected in advance. Local paths are derived for these MDL's as well as additional line segments, also connected to the same obstacle vertex, to show the object path with finer steps. It is easy to see that the underlying global path is also safe and smooth.

V. Conclusions and Future Works

In this paper, we propose a potential field model of the workspace which assumes object and obstacle boundaries are charged and thus re-

pelling one another. Such a potential model is more flexible than the one previously presented in [1] since nonuniform charge distributions are used in the modeling. The efficiency of the proposed approach is resulted from the existence of analytic expressions of the repulsion between two line segments, each being uniformly, linearly, or quardratically charged. A local planning procedure of deriving an object path of minimal potential is presented. According to the simulation results, improvements over the path planning results obtained with the uniform charge distribution, in terms of collision avoidance, path length, etc., can be achieved through proper selection of the nonuniform charge distributions along object/obstacle boundaries. Several path planning results involving multiple local paths are also presented. Similar path planning procedures for different types of workspace, e.g., a corridor in the free space, as well as applications of the proposed object/obstacle model to more general situations, e.g., for articulated objects and/or for nonstationary obstacles, are currently under investigation.

The proposed workspace model has the potential of accommondating certain constraints/considerations of interest to the underlying findpath problem, e.g., building material, protection measure, or uncertainty in location, which are generally nonuniform along workspace boundaries. However, the way to describe uncertainty or to weight protection may strongly depend on individual application. Thus, one of future research directions of such findpath problem is the derivation of proper charge distributions for objects and obstacles so that the nonuniform nature of their boundaries can be represented effectively.

REFERENCES

[1] J. H. Chuang and N. Ahuja, "An analytically tractable potential field model of free space and its application in obstacle avoidance," *IEEE Trans. Syst., Man, Cybern. B*, vol. 28, pp. 729–736, Oct. 1998.

[2] T. Lozano-Perez, "Automatic planning of manipulator transfer movements," *IEEE Trans. Syst., Man, Cybern.*, vol. SMC-11, pp. 681–698, Oct. 1981.

[3] T. Lozano-Perez, "Spatial planning: A configuration space approach," *IEEE Trans. Comput.*, vol. C-32, pp. 26–38, Feb. 1983.

[4] A. A. Maciejewski and J. J. Fox, "Path planning and the topology of configuration space," *IEEE Trans. Robot. Automat.*, vol. 9, pp. 444–456, Aug. 1993.

[5] M. Barbehenn and S. Hutchinson, "Efficient search and hierarchical motion planning by dynamically maintaining single-source shortest paths trees," *IEEE Trans. Robot. Automat.*, vol. 11, pp. 198–214, Apr. 1995.

[6] C. Laugier, F. D. I. Rosa, and J. Najera, "Robust path planning in the plane," *IEEE Trans. Robot. Automat.*, vol. 12, pp. 347–352, Apr. 1996.

[7] M. Herman, "Fast, three-dimensional, collision-free motion planning," presented at the Proc. IEEE Int. Conf. Robot. Automat., San Francisco, CA, Apr. 1986.

[8] S. R. Maddila, "Decomposition algorithm for moving a ladder among rectangular obstacles," presented at the Proc. IEEE Int. Conf. Robot. Automat., San Francisco, CA, Apr. 1986.

[9] S. Singh and M. D. Wagh, "Robot path planning using intersecting convex shapes," presented at the Proc. IEEE Int. Conf. Robot. Automat., San Francisco, CA, Apr. 1986.

[10] J. C. Zamiska, D. T. Kuan, and R. A. Brooks, "Natural decomposition of free space for path planning," presented at the Proc. IEEE Int. Conf. Robot. Automat., St. Louis, MO, Mar. 1985.

[11] J. S. B. Mitchell and C. H. Papadimitriou, "The weighted region problem: Finding shortest paths through a weighted planar subdivision," *J. ACM*, vol. 38, no. 1, pp. 18–73, Jan. 1991.

[12] O. Takahashi and R. J. Schilling, "Motion planning in a plane using generalized Voronoi diagrams," *IEEE Trans. Robot. Automat.*, vol. 5, pp. 143–150, 1989.

[13] A. Thanailakis, P. G. Tzionas, and P. G. Tsalides, "Collision-free path planning for a diamond-shaped robot using two-dimensional cellular automata," *IEEE Trans. Robot. Automat.*, vol. 13, pp. 237–250, Apr. 1997.

[14] C. E. Thorpe, "Path planning for a mobile robot," presented at the Proc. AAAI, Austin, TX, 1984.

[15] O. Khatib, "Real-time obstacle avoidance for manipulators and mobile robots," presented at the Proc. IEEE Int. Conf. Robot. Automat., St. Louis, MO, Mar. 1985.

[16] P. Khosla and R. Volpe, "Superquadric artificial potentials for obstacle avoidance and approach," presented at the Proc. IEEE Int. Conf. Robot. Automat., Philadelphia, PA, 1988.

[17] C. Diu, B. Cohen-Tannoudji, and F. Laloe, *Quantum Mechanics*. New York: Wiley, 1977, vol. 2.

[18] Y. K. Hwang and N. Ahuja, "Potential field approach to path planning," *IEEE Trans. Robot. Automat.*, vol. 8, pp. 23–32, 1992.

[19] J. Guldner and V. I. Utkin, "Sliding mode control for gradient tracking and robot navigation using artificial potential fields," *IEEE Trans. Robot. Automat.*, vol. 11, Apr. 1995.

[20] J. H. Chuang, "Potential-based modeling of three-dimensional workspace for obstacle avoidance," *IEEE Trans. Robot. Automat.*, vol. 14, pp. 778–785, Oct. 1998.

[21] J. Miura and Y. Shirai, "Vision and motion planning for a mobile robot under uncertainty," *Int. J. Robot. Res.*, vol. 16, no. 6, pp. 806–825, 1997.

Shape Partitioning by Convexity

Paul L. Rosin

***Abstract*—The partitioning of two-dimensional (2-D) shapes into subparts is an important component of shape analysis. This paper defines a formulation of convexity as a criterion of good part decomposition. Its appropriateness is validated by applying it to some simple shapes as well as against showing its close correspondence with Hoffman and Singh's part saliency factors.**

***Index Terms*—2-D shape analysis, decomposition, segmentation, visual perception.**

I. INTRODUCTION

A primary task in visual perception—for both biological and computer systems—is the analysis of shape. Despite its importance universal theories of shape have proven elusive, and much research continues to be carried out in a variety of disciplines including art [1], architecture [2], biological visual perception [3], psycholinguistics [4], qualitative reasoning [5], and computer vision [6]. One aspect of shape is the partitioning of a region into parts whose shapes are either simpler than the overall shape, or similar to an element from a predefined catalogue of primitive shapes [7]. Given the inherent difficulties of vision, particularly those related to the variability in the appearance of an object due to different viewpoints or articulation of parts, such a decomposition helps simplify the problem of perception. For instance, in many cases there will be a one-to-one correspondence between observable region parts and functional components of the viewed object.

Naturally image understanding involves a multitude of factors such as color, texture, shading, and motion, as well as nonvisual information such as contextual cues, prior expectations, etc. This paper is restricted to shape analysis, the importance and power of which was demonstrated by Biederman and Ju in experiments where both color pho-

Manuscript received April 2, 1999; revised October 31, 1999. This paper was recommended by Associate Editor J. Oommen.

The author was with the Department of Information Systems and Computing, Brunel University, Middlesex UB8 3PH, U.K. He is now with the Department of Computer Science, Cardiff University, Cardiff CF24 3XF, U.K. (e-mail: Paul.Rosin@cs.cf.ac.uk).

Publisher Item Identifier S 1083-4427(00)01730-6.